FAULT
JOURNAL

Open Access
Research Article
Received 6th April 2026
Accepted 11th April 2026

Hexagonally Ordered Silver Nanostructures from Polystyrene Colloidal Templates: Partial Success and Remaining Challenges

AUTHOR NAMES: Yuxin Yang[1, *]
[1]*Institute of Science Tokyo*
[*]*Corresponding author: 3010210978@qq.com*

Hexagonally ordered metallic nanostructures are of interest for optical and plasmonic studies because their response depends strongly on both local feature shape and long-range periodic arrangement. In this work, a polystyrene (PS) colloidal sphere self-assembly method is explored as a simple template-based route for fabricating hexagonally arranged Ag nanostructures. A PS monolayer is first assembled at the air–water interface and transfer onto a substrate, followed by Ag deposition, particle removal, and post-annealing treatment. Results show that locally ordered hexagonal packing could be obtained in small areas, but larger areas exhibit clear defects, including voids, domain misalignment, aggregation, and non-uniform coverage. After removal of the PS particles, periodic Ag patterns with sharp triangular vertex features are formed, reflecting the geometry of the interparticle gaps. Annealing further transforms these connected sharp features into more rounded and isolated island-like structures. These results confirm the basic feasibility of the method, while also revealing its current limitations in producing large-area, high-quality films.

KEYWORDS: Polystyrene colloidal spheres; Interfacial self-assembly; Hexagonal nanostructures; Silver nanostructures; Colloidal template; Annealing-induced morphology evolution

1 Introduction

Periodic metallic nanostructures have attracted broad interest because of their unique optical properties and their potential applications in plasmonics, sensing, light manipulation, and surface-enhanced spectroscopy[1–3]. In particular, hexagonally arranged nanostructures are useful because their periodic symmetry can produce characteristic responses under optical excitation, making them suitable platforms for studying structure-dependent electromagnetic behavior[2–4]. In many cases, not only the

individual feature shape but also the long-range arrangement of the array plays an important role in determining the final optical response[2–5]. Therefore, developing simple and controllable methods for fabricating large-area hexagonal metallic nanostructures remains an important topic[4–7].

Among the available fabrication methods, colloidal self-assembly using polystyrene (PS) microspheres is considered a simple and low-cost approach for preparing periodic templates[4–8]. When PS particles are arranged into a hexagonally close-packed monolayer, the interparticle gaps can serve as natural masks or molds for the subsequent deposition of metallic materials[4,5,8]. After metal deposition and removal of the colloidal particles, periodic metallic patterns can be left on the substrate[4,5]. In principle, this strategy provides a convenient route for producing ordered nanostructures without relying on expensive lithographic techniques[4,5,8]. In addition, further thermal treatment can modify the morphology of the deposited metal, providing another way to tune the final structure[9,10].

However, although the concept is straightforward, achieving a high-quality colloidal template over a large area is still challenging[6-8]. During interfacial self-assembly, the final film quality can be strongly affected by particle dispersion, solvent composition, surface-tension control, film transfer, and drying conditions. As a result, local ordering may be obtained in small regions, while defects such as voids, aggregation, and domain misalignment often appear when the observation area becomes larger. These defects can then be passed on to the final metallic structure, reducing its uniformity and limiting its usefulness in later optical studies[6,7]. For this reason, it is important not only to report successful structures, but also to record incomplete or imperfect results, since such observations can help clarify the limitations of the current process and guide later optimization[6,7].

In this work, a PS colloidal sphere self-assembly method is investigated for the fabrication of hexagonally arranged Ag nanostructures. The assembly behavior of the PS template is first examined by AFM and SEM, followed by Ag deposition, removal of the PS particles, and post-annealing treatment. The results show that the present method can generate locally ordered hexagonal arrangements and can transfer the interparticle geometry of the colloidal template into metallic patterns with triangular vertex features[4,5]. Annealing further changed these connected sharp structures into more rounded and isolated islands[9,10]. At the same time, the experiments also reveal clear problems in large-area film quality, including gap formation, domain mismatch, aggregation, and non-uniform coverage[6–8]. Therefore, this study serves not only as a demonstration of the basic feasibility of the method, but also as a record of its present limitations, providing useful information for future improvement of large-area ordered metallic nanostructures.

2 Experiment

A total of 250 μL of a PS colloidal suspension with a particle diameter of 500 nm was first centrifuged to remove the original aqueous medium. After removal of the supernatant, the precipitated PS particles were redispersed in a mixed solvent containing 100 μL ethanol and 10 μL ethylene glycol by shaking. The reconstituted suspension was then used for interfacial self-assembly.

A circular glass slide was cleaned with ethanol and deionized water, and 30 μL of the PS suspension

was dropped onto its surface. The slide was gently shaken to spread the suspension uniformly, and then slowly brought into contact with the surface of pure water. Owing to the difference in solvent composition and surface tension, the suspension spontaneously spread over the air–water interface, forming a floating monolayer of PS particles. After standing for 5 min, 0.8 mL of 10% sodium dodecyl sulfate (SDS) solution was added dropwise to the water surface. The resulting surface-tension-driven compression induced the PS particles to rearrange into a hexagonally close-packed monolayer. The film was allowed to stabilize for an additional 10 min.

The assembled PS monolayer was subsequently transferred onto a glass substrate pretreated by ethanol cleaning, deionized water rinsing, and plasma treatment. After drying naturally, an ordered PS colloidal template was obtained. A 30 nm silver layer was then deposited onto the template by thermal evaporation, followed by removal of the PS particles using tape, yielding a periodic Ag nanostructure with hexagonal ordering. The as-prepared structure exhibited curved triangular features at the vertices of the hexagonal units. To further modify the morphology, the sample was annealed at 500 °C for 8 h in air under a reduced pressure of approximately 10^{-3} in a hard glass tube. After annealing, the triangular vertex features gradually evolved into rounded sphere-like structures, leading to the formation of a regular hexagonally ordered Ag nanostructure array.

Figure 1. Illustration of the whole experimental process. This illustration is generated by AI.

3 Result

This section presents the erroneous data collected in this study, including data anomalies caused by human error, instrument failure, operational deviation, or other unexpected factors. All invalid, abnormal, or faulty data are clearly displayed and recorded as part of the research process.

To evaluate the feasibility and limitations of the presented method, the samples were characterized by atomic force microscope (AFM) and scanning electron microscope (SEM) before metal deposition. As shown in Figure 2, panels a–c present the AFM images with scan areas of 5 × 5 μm², 10 × 10 μm², and 20 × 20 μm², respectively, while panels d–f show the corresponding SEM images recorded at magnifications of 20,000×, 12,000×, and 6,000×. Overall, these results indicate that the present method can produce locally ordered hexagonally close-packed domains on a small scale; however, as the observation area increases, structural defects become progressively more evident, demonstrating that the current process is still insufficient for the reliable fabrication of large-area, highly ordered colloidal templates.

From the AFM results, the 5 × 5 μm² image in Figure 2a shows that the PS microspheres possess relatively uniform size and clear spherical shapes. In this local region, the particles are closely packed and exhibit an obvious tendency toward hexagonal close packing. The center-to-center spacing between neighboring particles is relatively uniform, indicating that the combination of solvent exchange (changed from water to a mixture of ethanol and ethylene glycol) and surface-tension-induced compression (due to SDS solution) is effective, at least on a local scale, in driving the colloidal particles to rearrange into an ordered two-dimensional array. Therefore, the present assembly strategy is capable of generating reasonably well-ordered domains within a limited area.

When the scan area is increased to 10 × 10 μm², as shown in Figure 2b, the surface still retains some periodic arrangement; however, defects become more clearly. In addition to locally ordered regions, particle misalignment, discontinuous domain boundaries, and several abnormal regions can already be observed. These features indicate that, during the self-assembly process, the particles do not rearrange themselves in a completely simultaneous and uniform manner across the entire surface. Instead, the film consists of multiple locally ordered small domains. When these domains expand and come into contact with one another, orientational mismatch occurs at their boundaries, resulting in dislocations and misaligned packing.

In the larger 20 × 20 μm² scan shown in Figure 2c, these problems become even more pronounced. Although some regions still preserve the characteristics of hexagonal ordering, the overall continuity and uniformity of the colloidal film are clearly reduced. Significant gaps, mismatched domain connections and localized particle clusters can be observed. These results indicate that the present method is unable to maintain a continuous and well-ordered monolayer over a larger area. In particular, the appearance of gaps and sparse regions suggests that the surface is not completely covered by particle during the colloid spreading, compression, or transfer processes. Meanwhile, the particle

clusters imply that the colloids are not perfectly dispersed as a single layer. These defects can reduce the quality of the colloidal template and may affect the uniformity and reproducibility of the nanostructures formed in the following steps.

The SEM observations further support the AFM analysis. In the high-magnification SEM image (Figure 2d, 20,000×), the particles still exhibit relatively regular hexagonal close packing within a limited observation region, confirming that the current method can indeed generate locally ordered structures. However, in the medium- and low-magnification SEM images (Figure 2e, 12,000×; Figure 2f, 6,000×), the accumulation of defects with increasing observation area becomes much more apparent. In addition to locally ordered domains, the sample surface exhibits obvious gaps, disordered packing regions, misaligned boundaries between neighboring domains, and abnormal areas caused by particle clusters. These observations indicate that the sample do not form a continuous large-area single-crystal-like colloidal film, but rather a polycrystalline two-dimensional particle layer composed of multiple small ordered domains.

It should be noted that, because the PS colloidal particles are non-conductive, a thin conductive metal coating was deposited on the sample surface before SEM observation in order to improve image quality and suppress charging effects. As a result, the interparticle gaps in Figures 2e and 2f are less clearly resolved, which may visually give the impression that neighboring particles are connected or even fused together. However, this effect mainly arises from the conductive coating and the resulting reduction in topographical contrast, rather than from actual fusion of the colloidal particles. In combination with the AFM results, it can still be concluded that the sample surface is composed of spherical particles, although the interparticle boundaries become more difficult to distinguish under low magnifications.

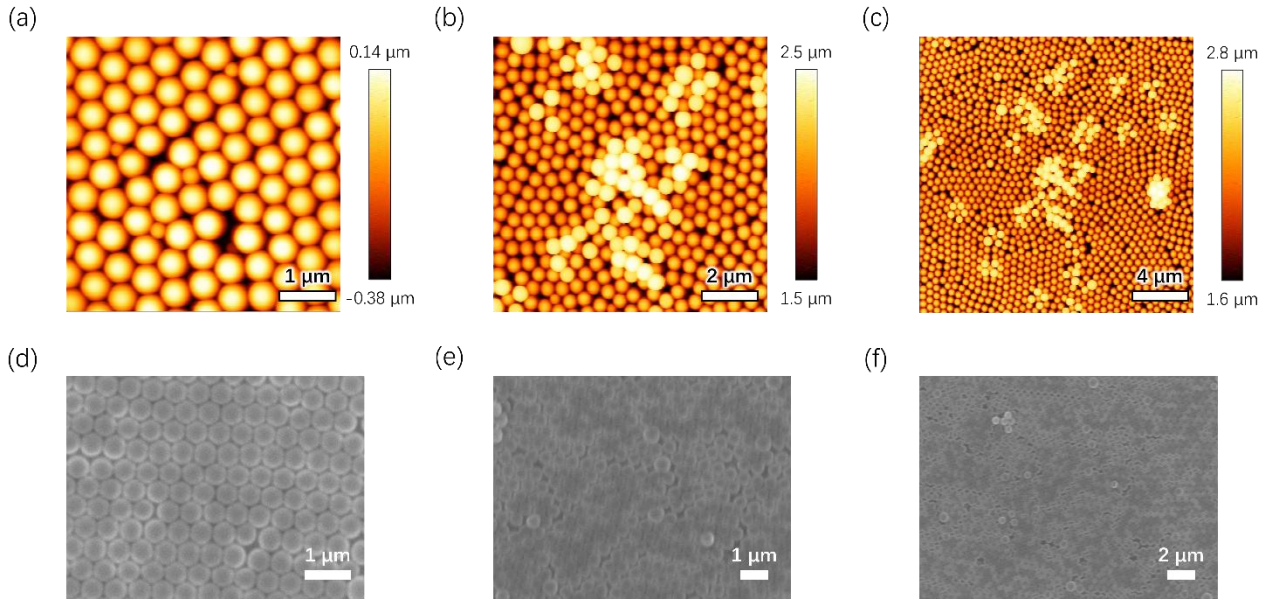

Figure 2. Surface morphology of the sample before Ag deposition and removal of the PS colloidal particles by tape. AFM images with the scan area of 5 × 5 μm² (a), 10 × 10 μm² (b) and 20 × 20 μm², respectively. SEM images taken at magnifications of 2,0000× (d), 12,000× (e) and 6,000× (f),

respectively.

Figure 3 shows the surface morphology of the sample after Ag deposition and removal of the PS colloidal particles by using tape. Figure 3a is the AFM image with a scan area of 5 × 5 μm², while Figures 3b and 3c are SEM images taken at magnifications of 12,000× and 6,000×, respectively. Compared with the sample before particle removal, the surface no longer shows a continuous array of spherical particles. Instead, it displays a two-dimensional metallic pattern with periodic features, indicating that the deposited silver remains in the spacing between the colloidal particles and forms the corresponding nanostructure after the colloidal film is removed.

The AFM image clearly shows a relatively regular hexagonal arrangement on the surface, and the vertices of each unit exhibit sharp triangular features. This shape is closely related to the geometry of the gaps formed between the PS particles in the hexagonally close-packed template. In a monolayer of closely packed spheres, triangular gaps are formed between every three neighboring particles. During sliver deposition, the metal is deposited not only on the tops of the particles but also into these interparticle gaps. After the PS particles are removed by tape, the silver deposited in the triangular gaps remains on the substrate. As a result, sharp triangular structures appear at the vertices of the hexagonal pattern. This indicates that the geometry of the final metal pattern is directly determined by the shape of the gap in the colloidal template.

The SEM images further reveal the actual quality of the structure over a larger area. In Figure 3b, some local regions still show a certain degree of periodic ordering, suggesting that the target pattern can be reproduced on a small scale. However, the arrangement is not continuous and is far from ideal. Clear domain boundaries can be observed between neighboring ordered regions, and the packing direction is not consistent from one domain to another, leading to misalignment at the boundaries. In addition, the cluster of particles or metallic structures is also present, causing irregular feature size and spacing in some areas. Figure 3c, which covers a larger area, shows that these problems are not isolated cases but are widely distributed over the entire film. Besides domain misalignment and cluster, the overall uniformity of the film is poor, and the structural quality varies strongly from region to region. Some abnormal features can also be observed locally, indicating that the resulting metallic film is not of high quality.

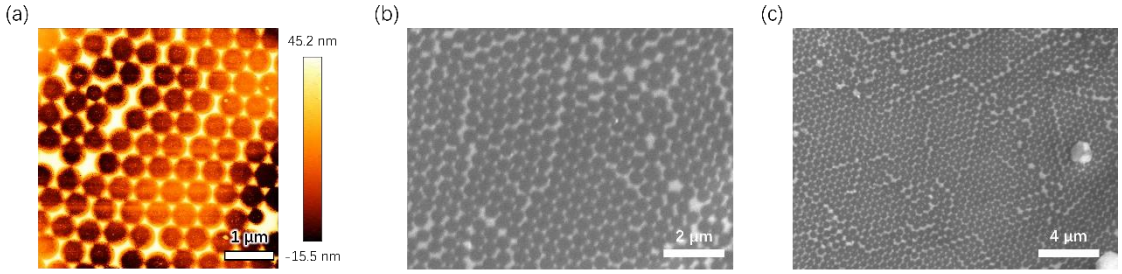

Figure 3. Surface morphology of the sample after Ag deposition and removal of the PS colloidal particles by tape. (a) AFM image with a scan area of 5 × 5 μm². (b, c) SEM images taken at magnifications of 12,000× and 6,000×, respectively.

Figure 4 shows the surface morphology of the sample after annealing. Figure 4a is the AFM image with a scan area of 5 × 5 μm², while Figures 4b and 4c are SEM images taken at magnifications of 12,000× and 6,000×, respectively. As is often the case in nanoscale studies, some structures, like brief encounters in life, are difficult to revisit once missed. Therefore, the observation positions in Figure 4 are not exactly the same as those in Figure 3, and the images are not taken from the identical sample piece; the main point is the morphological evolution after annealing.

The AFM image (Figure 4a) shows that the structure changed clearly after annealing compared with the unannealed sample. The most obvious change is that the sharp triangular features originally located at the vertices of the hexagonal units become much less pronounced, and the overall shape become more rounded. This suggests that during heat treatment, the silver structures experience clear surface diffusion and rearrangement. Driven by surface energy, the metal features with sharp corners gradually change into smoother and more stable shapes. At the same time, the original connections between neighboring vertices are broken because of metal migration, leading to the formation of separated island-like structures. This change is meaningful for later optical or electromagnetic studies. On one hand, after the vertices become more rounded, the response is no longer too strongly concentrated only at extremely sharp tips. This can reduce the strong local effect that exists mainly at the tip and allow more of the response to come from the periodic structure itself. On the other hand, the island-like separation blocks the connection between neighboring vertices, which helps confine the response to each individual vertex or local unit instead of a large connected metal region. As a result, the structural response is expected to become clearer and easier to analyze.

The SEM images further confirm this annealing-induced change in morphology. Figure 4b shows that, in a local region, the previously connected vertex structures have become clearly separated and now appear as nearly round particles distributed at periodic positions. Figure 4c shows the same island-like feature over a larger area, indicating that the annealing treatment affects the whole sample surface.

However, it should be emphasized that, although the annealing step itself is successful and clearly changes the structure from sharp connected features into rounded isolated islands, the overall film quality is not fundamentally improved. As seen in Figures 4b and 4c, the film remains obviously non-uniform over a large area. The size, spacing, and completeness of the structures vary from region to region, and many local defects are still present. Therefore, the present results show that annealing successfully changed the morphology of the silver nanostructure, but they do not indicate that a high-quality, large-area, uniform metallic nanofilm has been achieved. Further improvement of the initial colloidal template and the overall fabrication process is still necessary.

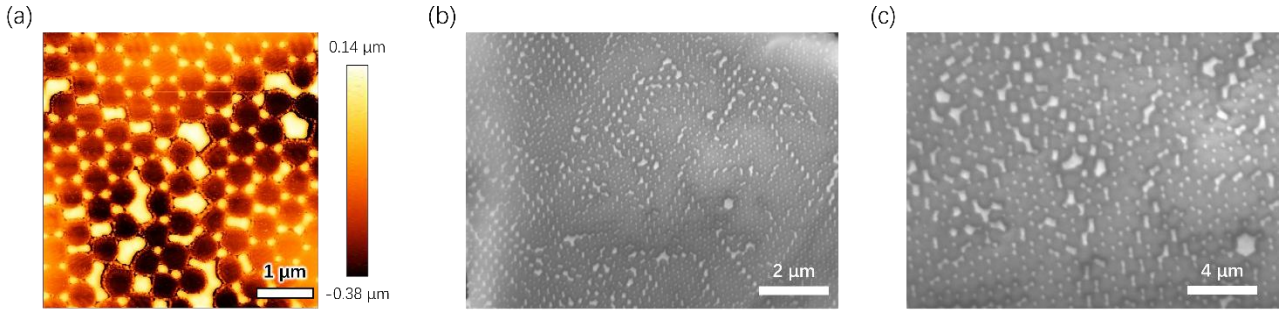

Figure 4. Surface morphology of the sample after annealing. (a) AFM image with a scan area of 5 × 5 μm². (b, c) SEM images taken at magnifications of 12,000× and 6,000×, respectively.

Figure 5 shows the dispersion behavior of the samples under transmitted light. In this test, a light source was placed below the sample, and the color distribution of the transmitted light was observed from the upper side of the sample. Figure 5a corresponds to the sample after Ag deposition but before removal of the PS colloidal particles by tape, while Figure 5b corresponds to the sample after Ag deposition and after removal of the PS particles. As can be seen, both samples show visible color responses, indicating that their surface micro/nanostructures are able to modulate the incident light. However, there is a clear difference in color intensity between the two cases. The color in Figure 5a is deeper and more saturated, whereas the color in Figure 5b is much lighter, suggesting a weaker overall dispersion effect.

This difference is most likely related to the size of the structures that actually interact with light on the sample surface. In Figure 5a, the PS colloidal particles are still present on the glass substrate, so the main structural feature is still the array of spherical particles with a diameter of about 500 nm. This size is close to the wavelength range of visible light and can therefore produce stronger scattering, diffraction, and interference effects. As a result, the transmitted light shows a more obvious dispersion behavior. In addition, this larger particle-based structure has a higher surface coverage and a more pronounced three-dimensional topography, which can further increase the difference in optical path and make the observed colors stronger.

In contrast, in Figure 5b, the PS colloidal particles have already been removed, and only the Ag nanostructures deposited in the gaps between the particles remain on the surface. Because the deposited Ag thickness was only 30 nm, the characteristic size of the remaining structures is much smaller than that of the original 500 nm colloidal particles. Although the lateral size is not necessarily exactly 30 nm, the surface structure has clearly changed from a submicron spherical array to a much smaller metallic pattern. As the structural size becomes smaller, the ability of the sample to geometrically modulate visible light is also reduced. Therefore, the scattering and diffraction effects in transmitted light become weaker, which is consistent with the lighter color and weaker dispersion seen in Figure 5b.

In addition, the two samples are also different in structural continuity and morphology. Figure 5a still contains the full three-dimensional colloidal particle array, while Figure 5b mainly consists of a thinner two-dimensional metallic pattern left on the substrate. These two types of structures differ in effective

refractive index distribution, surface roughness, and local light-field distribution, all of which can influence the transmitted color. Therefore, the difference in color depth between Figures 5a and 5b not only reflects the change in structural size but also suggests that the optical response changes clearly when the surface structure changes from a full colloidal particle array to a residual metallic nanostructure.

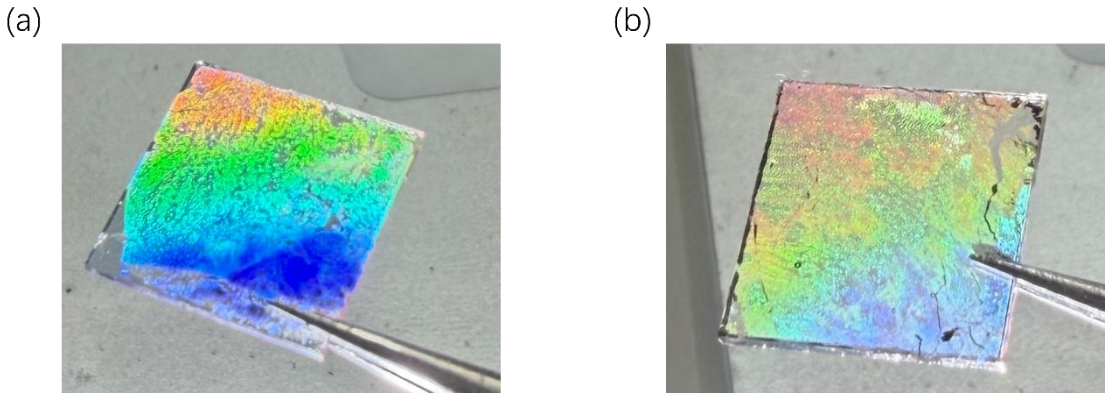

Figure 5. Images showing the dispersion behavior of the samples under transmitted light. The light source was placed below the sample, and the transmitted light was observed from the upper side. (a) Sample after Ag deposition without removal of the PS colloidal particles. (b) Sample after Ag deposition and removal of the PS particles by tape.

4 Conclusion

In this study, a PS colloidal sphere self-assembly method is explored for the fabrication of hexagonally arranged Ag nanostructures. The results show that the present process can produce locally ordered hexagonal packing on a small scale, indicating that the basic assembly strategy is workable. After Ag deposition and removal of the PS particles, periodic metallic patterns with sharp triangular vertex features are obtained, reflecting the geometry of the interparticle gaps in the original colloidal template. Subsequent annealing successfully change these sharp connected features into more rounded and isolated island-like structures, confirming that thermal treatment is an effective way to tune the final morphology.

At the same time, the overall film quality remain far from ideal. Although local ordering is observed, AFM and SEM results consistently showed that defects become more obvious as the observation area increased. Gaps, domain misalignment, aggregation, and non-uniform coverage are widely present, and these defects are transferred into the final metallic structures. Therefore, the present work demonstrates a partial success in structure formation, but also clearly shows that the current method is not yet sufficient for the reproducible fabrication of large-area, high-quality hexagonal Ag nanostructures. Further optimization of the colloidal assembly and transfer process is still required. Nevertheless, despite the structural imperfections and the limitations of the present fabrication method, the sample still displayed a striking rainbow-like color under transmitted light, leaving a strong visual impression and suggesting considerable optical potential.

Reference

[1] Yu, H.; Peng, Y.; Yang, Y.; Li, Z.-Y. **Plasmon-enhanced light–matter interactions and applications.** *npj Computational Materials* **2019**, *5*, 45.

[2] Anker, J. N.; Hall, W. P.; Lyandres, O.; Shah, N. C.; Zhao, J.; Van Duyne, R. P. **Biosensing with plasmonic nanosensors.** *Nature Materials* **2008**, *7*, 442–453.

[3] Maier, S. A. **Plasmonics: Fundamentals and Applications**; Springer: New York, 2007.

[4] Hulteen, J. C.; Van Duyne, R. P. **Nanosphere lithography: A materials general fabrication process for periodic particle array surfaces.** *Journal of Vacuum Science & Technology A* **1995**, *13*, 1553–1558.

[5] Haynes, C. L.; Van Duyne, R. P. **Nanosphere lithography: A versatile nanofabrication tool for studies of size-dependent nanoparticle optics.** *The Journal of Physical Chemistry B* **2001**, *105*, 5599–5611.

[6] Lotito, V.; Zambelli, T. **Approaches to self-assembly of colloidal monolayers: A guide for nanotechnologists.** *Progress in Surface Science* **2017**, *92*, 184–202.

[7] van Dommelen, R.; Fanzio, P.; Sasso, L. **Surface self-assembly of colloidal crystals for micro- and nano-patterning.** *Advances in Colloid and Interface Science* **2018**, *251*, 97–114.

[8] Ye, X.; Qi, L.; Huang, X.; et al. **Monolayer Colloidal Crystals by Modified Air–Water Interface Self-Assembly Approach.** *Nanomaterials* **2017**, *7*(10), 291.

[9] Preston, A. S.; Hughes, R. A.; Demille, T. B.; Rey Davila, V. M.; Neretina, S. **Dewetted nanostructures of gold, silver, copper, and palladium with enhanced faceting.** *Acta Materialia* **2019**, *165*, 15–25.

[10] Hulteen, J. C.; Treichel, D. A.; Smith, M. T.; Duval, M. L.; Jensen, T. R.; Van Duyne, R. P. **Size-Tunable Silver Nanoparticle and Surface Cluster Arrays.** *The Journal of Physical Chemistry B* **1999**, *103*(19), 3854–3863.